University of Nevada, Reno

Abnormal cell patterning at the cortical gray-white matter boundary in

autism spectrum disorders

A thesis submitted in partial fulfillment of the requirements for the degree of Master of

Arts in Psychology

by

Thomas A. Avino

Dr. Jeffrey J. Hutsler/Thesis Advisor

May, 2011

THE GRADUATE SCHOOL

University of Nevada, Reno
Statewide • Worldwide

We recommend that the thesis
prepared under our supervision by

THOMAS A. AVINO

entitled

Abnormal Cell Patterning At The Cortical Gray-White Matter Boundary In Autism Spectrum Disorders

be accepted in partial fulfillment of the
requirements for the degree of

MASTER OF ARTS

Jeffrey J. Hutsler, Ph.D., Advisor

Michael A. Crognale, Ph.D., Committee Member

Grant S. Mastick, Ph.D., Graduate School Representative

Marsha H. Read, Ph. D., Associate Dean, Graduate School

May, 2011

Abstract

Previous research on neuronal spacing and columnar organization indicates the presence of cell patterning alterations within the cerebral cortex of individuals with autism spectrum disorders (ASD). These patterning abnormalities include irregularities at the gray-white matter boundary and may implicate early neurodevelopmental events such as migration in altering cortical organization in ASD. The present study utilized a novel method to quantify the gray-white matter boundary in eight ASD and eight typically developing control subjects. Digital photomicrographs of the gray-white matter boundary were acquired from multiple positions within the superior temporal gyrus (BA 21), dorsolateral frontal lobe (BA 9), and dorsal parietal lobe (BA 7) of each case. A sigmoid curve was fitted to the transition zone between layer VI and underlying white matter (subplate), and the slope of the resulting curve was used as a measure of the spatial extent of the transition zone. For all three cortical regions examined, ASD subjects showed "shallower" sigmoid curves compared to neurotypicals, indicating the presence of an indistinct boundary between cortical layer VI and the underlying white matter. These results may reflect the presence of supernumerary neurons beneath the cortical plate that could be the result of migration deficits or failed apoptosis in the subplate region. Furthermore, these findings raise questions regarding the validity of cortical measures that rely on gray-white matter parcellation, since an indistinct transition zone could lead to a misplaced cortical boundary and errors in both thickness and volume measures.

Acknowledgements

Table of Contents

List of Tables

List of Figures

1. Introduction

Autism spectrum disorders (ASD) are a family of developmental disabilities characterized by impairments in social interaction, delayed or absent language development, and restricted or repetitive behaviors and interests (Rapin, 1997). Investigations of this disorder point to a neurodevelopmental origin; however, a clear biological marker for autism is not currently available. Several studies have documented both gross and microanatomical changes to the cerebral cortex that may result in increased brain size, changes to cortical thickness, alterations to gray and white matter volumes, connectional alterations, and changes to the cell patterning found in neurotypical controls (Casanova et al., 2002; Bailey et al., 1998; Hutsler et al., 2007; Hutsler & Zhang 2010). The developmental processes that bring about these organizational changes remain largely unidentified, but several authors have suggested that migration problems during early gestation may play a prominent role. Cell migration abnormalities in ASD were initially suggested based upon descriptions of cell patterning abnormalities within the cerebellum (Bauman & Kemper 1985; Kemper 1988), as well as cerebellar abnormalities that were identified in magnetic resonance imaging (MRI) studies (Courchesne, 1988). Cerebral cortical migration deficits in individuals with ASD were subsequently suggested based upon structural abnormalities found in MRI studies (Piven et al., 1990).

Perhaps the strongest support for migration abnormalities in ASD is the abnormal expression of migration-relevant neurochemicals. ASD subjects show high rates of dysfunction in the gene for reelin, which plays an important role in both neuronal migration and cortical layering within the cerebral cortex (Fatemi et al., 2005; Skaar et

al., 2005; Zhang et al., 2002; Serajee, Zhong, & Huq, 2006; Fatemi, Stary, & Egan, 2002). Similarly, Janusonis, Gluncic, and Rakic (2004) have examined the role of the serotonergic system in cortical development in the mouse and have shown that manipulations of this system can influence both cortical patterning and reelin expression. Markers of abnormal serotonin expression found throughout development in ASD may, therefore, also have implications for migration disorders in autism (Chugani, 2004).

Despite the evidence for abnormal cell patterning from both postmortem neuroanatomical studies and examinations of migration-relevant neurochemicals, one does not see the type of cortical disarray that is found in, for example, reelin knock-out mice (Rice and Curran, 2001). Instead, the cortex shows a quantitatively normal layering pattern and a limited set of restricted organizational abnormalities that can include high neuronal densities, supernumerary neurons in the molecular layer, small areas of neuronal disorganization, neuronal heterotopias, and, most relevant to the present study, poor differentiation of the gray-white matter boundary along with supernumerary neurons in the subcortical white matter (Casanova et al., 2002; Bailey et al., 1998; Hutsler et al., 2007; Simms et al., 2009). The origin of subcortical white matter neurons in ASD has yet to be determined. In addition to speculations about migration, some researchers suggest that this abnormality could be due to the retention of transient subplate neurons within the subcortical white matter (Chun & Shatz, 1989; Kemper, 2010). Despite these descriptions, there has never been a systematic neuroanatomical examination of the gray-white matter transition zone in ASD.

In addition to its relevance to migration, the transition zone between gray and white matter is also pragmatically relevant to MRI studies of the cerebral cortex that rely

on tissue parcellation. Differences in cell patterning at the gray-white matter transition zone are likely to influence MRI intensity values and the subsequent, algorithm-dependent placement of the lower boundary of the cortex. Results from studies examining *volume* in ASD are mixed, with findings of increased cortical volume, volume decreases, and no differences between ASD subjects and neurotypicals (Courchesne et al., 2001; Hazlett et al., 2005; Hazlett et al., 2006; Palmen et al., 2005; Herbert et al., 2003; McAlonan et al., 2008; Bonhila et al., 2008; Frietag et al., 2009; Hallahan et al., 2009; Harden et al., 2001; Rojas et al., 2002; Boddaert et al., 2004).

Although measures of cortical thickness are less common in the literature, cortical thickening has been reported in ASD (Harden et al., 2006). But, like the literature on cerebral volume, other studies show only slight or no thickening (Hutsler et al., 2007) or a decrease in cortical thickness (Chung et al., 2005; Hadjikhani et al., 2006). Naturally, variability in the results of both volumetric and thickness measures may be explained by the specific methodology employed, the specific regions examined, the nature of the ASD sample, or some combination of these factors.

In the present study, we employed a novel methodology to quantify the abruptness of the transition zone between the gray and white matter from eulaminate isocortex (Bailey and von Bonin, 1951) in frontal, parietal, and temporal locations. Sigmoid functions were used to model the abruptness of the transition in order to determine if systematic differences in cell patterning at this boundary might be present in ASD subjects. Such differences may indicate early alterations to the prenatal development of the cortex in the form of either migration deficits, alterations in apoptosis, or differences in other developmental factors that influence cell patterning.

Furthermore, if early cell patterning events are the source of abnormalities at this boundary, we predict that they will not be regionally specific.

2. Results

The transition zone between gray and white matter was found to be less clearly delineated in ASD subjects compared to typically developing controls as evidenced by higher slope values in ASD (i.e., shallower slopes) for the sigmoid functions that were fit to the boundary ($F[1,26.8] = 6.4$, $p = .017$; see figures 1 and 2). For each region examined, ASD subjects had shallower gray-white matter transition boundaries relative to typically developing subjects. Slope values acquired from three regions of eulaminate isocortex taken from three cortical lobes (BA7, BA9, and BA21) did not differ from each other ($F[2,25.1] = 1.15$, NS) and, in addition, cortical region did not interact with subject diagnosis ($F[2,25.1] = .41$, NS; see figure 2).

Although positive relationships between the sigmoid slope values and age ($r = .399$, NS), postmortem interval (PMI; $r = .280$, NS), and brain weight ($r = .45$, NS) were found, they were never reliable in this small sample. To further explore their impact on the differences between ASD and typically developing subjects, these variables were also included as covariates in the mixed model analysis both singly and in combination. In each of these analyses the pattern of results remained unchanged: ASD subjects always showed significantly shallower slope values relative to typically developing subjects, while both region and the interaction between region and diagnosis were nonsignificant.

Because assessments of the transition zone could be nonsystematically affected by measures that are not perfectly orthogonal to the gray white matter boundary, the influence of two potential sources of measurement error were also explored. The first was

the in-plane tilt of the gray-white matter boundary. Images were initially acquired so that the gray-white matter boundary was perpendicular to the long axis of the image; however, there was no practical way to systematically ensure the precision of this orientation. To both measure and correct for orientation error, we used multiple sigmoid functions that were fit to the transition zone every 150 micrometers (i.e., six per image). A linear fit was generated to the offset values of these sigmoids to automatically find the boundary in each image. Although the absolute angle of tilt as assessed by this measure was typically small ($\bar{x} = 3.76° \pm 1.08°$) and did not differ systematically between ASD and control cases (t[14] = .122, NS), these measures were applied to the raw sigmoid slope values as a correction. As expected, the pattern of results was unchanged. Slope values continued to differ between ASD and neurotypical subjects (F[1,30.0] = 8.2, p = .007) while neither region (F[2,23.2] = 0.48, NS) nor the interaction between region and diagnosis (F[2, 23.1] = 0.07, NS) were significant.

The second potential source of measurement error is similar to the first but concerns tilt that occurs out of the image plane that is due to variation in the angle of cut. Although we attempted to cut all tissue blocks orthogonal to the cortical surface, it is possible that an oblique angle of sectioning could result in shallower sigmoid slopes. As a result, sigmoid slopes from every image were also corrected for out of plane errors as assessed by cortical thickness measures.

$$CorrectedSlope = SigmoidSlope(a/b)$$

Here *a* represents the smallest cortical thickness measurement in a subject case for a particular region, and *b* represents the actual cortical thickness measure taken at the location where a specific image was acquired. Although this correction is not ideal,

because it assumes that the tissue section with the smallest thickness was cut perpendicular to the cortical surface, it does attempt to reduce nonorthogonal cutting error within a single tissue block. Correcting the sigmoid slope for cortical thickness did not change the pattern of results as indicated by a significant main effect ($F[1, 21.8] = 8.2$, $p = .009$), and no effect of region ($F[2, 23.5] = 1.6$, NS) or an interaction between region and diagnosis ($F[2, 23.3] = .41$, NS).

To explore the subject characteristics of our sample, bivariate correlations between age, brain weight, PMI and diagnosis were considered. Only age and brain weight were reliably associated with each other ($r = .52$, $p < .05$; table 2), and, as indicated previously, correlations between these variables and the sigmoid slope of the gray-white matter transition zone never reached significance. In addition to quantitative considerations of age, PMI, and brain weight, we also considered several other *qualitative* characteristics in individual subjects including their general level of cognitive functioning and any history of seizure activity. Seven of the eight individual ASD subjects in this study showed shallower sigmoid slope angles relative to the mean of the neurotypicals ($z = -.61$ to -3.44; see figure 3), while the one remaining ASD subject showed a positive z value ($+.71$) relative to the neurotypical subjects. This autistic subject was described as being severely mentally retarded without a history of seizure activity. Seven of the eight subjects had some degree of mental retardation, while one subject, who was diagnosed as having Asperger's, was high functioning with normal full-scale IQ measurements. This highest functioning case had a history of seizures and a z value relative to neurotypicals of -1.89, which was comparable to several other autistic cases with mild to moderate mental retardation. Only one other case had a documented history

of seizure activity, and this subject also showed a shallower transition zone relative to the mean of the control group ($z = -1.98$). In sum, level of cognitive functioning did not appear to relate in a systematic manner to the average slopes found at the gray-white matter boundary in individual cases, and although both cases with a documented history of seizures had shallow slope values, these were not dissimilar from the other ASD subjects.

3. Discussion

Using a novel method for gray-white matter boundary quantification, we have shown that the subcortical boundary is less distinct in subjects with autism spectrum disorders relative to neurotypical control subjects. To our knowledge this is the first postmortem tissue study in ASD individuals to attempt to quantify this cell patterning abnormality at the gray-white matter transition zone. Although substantial group differences between typical subjects and controls were found, like previous neuropathological studies in autism (for example, Simms et al., 2009; Whitney et al., 2008) not every case reliably demonstrated the effect, An examination of subject characteristics that might distinguish between subgroups of ASD patients did not reveal a salient pattern.

3.1 Cell Patterning at the Gray-White Matter Boundary

Neurons that extend into the cortical subplate region could have several potential origins during development. Here we describe three hypotheses. First, these neurons could be the result of incomplete neuroblast migration into the cortical plate during prenatal development. Migration deficits in ASD individuals were first proposed based upon evidence from the cerebellum (Bauman and Kemper 1985; Kemper, 1988).

Following this, cerebral cortical migration deficits were proposed based upon MRI evidence (Piven et al., 1990) and have been qualitatively supported in a subset of postmortem cases where increased neurons have been found in the subplate region (Bailey, 1998; Hutsler et al., 2007). As discussed, reelin and serotonin expression, which both play a role in cortical migration, are also abnormally expressed in ASD cases (Fatemi et al., 2005; Skaar et al., 2005; Zhang et al., 2002; Serajee, Zhong, & Huq, 2006; Fatemi, Stary, & Egan, 2002; Janusonis, Gluncic, & Rakic, 2004). Unlike the previous qualitative descriptions of this phenomenon in ASD subjects that indicate only a subset of subjects have supernumerary cell in this region, the present work shows a quantifiable alteration in seven of the eight ASD subjects examined. Notably, migration problems have also been associated with the diagnosis of epilepsy (Rice and Barone, 2000; Battaglia et al., 1996). Although epilepsy and ASD are highly comorbid (Canitano, 2007), in the present study there did not appear to be a consistent relationship between cell patterning abnormalities at the gray-white matter transition zone and a history of seizure activity, although the two cases that did have comorbid seizures did have shallower slopes relative to the control group. In addition, it should be noted that hypotheses that posit migration anomalies in ASD subjects must be reconciled with the limited abnormalities found in cell patterning and layering within the cerebral cortex in ASD (Hutsler et al., 2007). Thus, if a migration anomaly is a consistent characteristic in ASD cases, it must be limited in its scope given the qualitatively unremarkable appearance of cerebral cortical histology.

The second hypothesis that might explain abnormal cell patterning in ASD is that there may be incomplete apoptosis of neurons in the subplate region. In humans, subplate

neurons have their origin in the lower portion of the primoridal plexiform layer, which is present at the outer wall of the neural tube prior to the arrival of the first neuroblasts that will form the cortical plate (MarinPadilla, 1998). Neurons in the subplate play a role in guiding cortical development, particularly with regard to connections to the thalamus (McConnell, Ghosh, & Shatz, 1994), and it has been suggested that the majority of these neurons die after migration is complete (Al Ghoul & Miller, 1989; Chun & Shatz, 1989). If this is true, then the retention of transient cell populations in both the subplate and layer I in ASD subjects might indicate incomplete apoptotic processes that would then contribute to the less distinct gray-white matter boundary (Kemper, 2010).

Finally, an indistinct boundary between the cortical ribbon and the subplate could be the result of modifications to other factors that affect cell patterning in the developing cortex. Altered neurochemical expression, gene expression, neuronal activity, calcium signaling, and glial cells have all been shown to participate in cell patterning and could potentially affect boundary-related cell patterning in ASD subjects (e.g., Nomura et al., 2008; Puelles & Rubenstein, 2003; Mennerick & Zorumski, 2000; Bushong et al., 2003). Factors such as abnormal genetic and neurochemical expression may be especially relevant in ASD (Muhle et al., 2004; Newshaffer et al., 2007). Importantly, cell to cell interactions between reelin expressing Cajal Retzius cells and arriving neuroblasts are thought to be responsible for the boundary that is found between the cell-sparse layer I and the adjacent cell-dense layer II (Marin-Padilla, 1998). Similar interactions between subplate neurons and layer VI cell may also play an important role in cell patterning at the gray-white matter boundary (Hevner et al., 2001).

3.2 Cell Patterning and Boundary Placement

Beyond the neurodevelopmental implications of abnormal cell patterning at this cortical boundary, cell patterning alterations may also influence measures of cortical thickness and cortical volume. In MRI studies, Harden et al. (2006) showed that individuals with autism display an increase in cortical thickness in the temporal lobe. Cortical thickening has also been reported in postmortem tissue studies (Bailey 1998); however, the magnitude of this effect appears to be small (Hutsler et al., 2007). Cortical thinning has also been reported, but this finding is most typical in voxel-based morphometry (VBM) studies (McAlonan et al., 2005; McAlonan et al., 2008; Boddaert et al., 2004). Other studies have also reported thinning of the autistic cortex (Chung & Robbins, 2005; Hadjikhani et al., 2006). Most studies that have examined the volume of gray matter in autism report increased volume compared to neurotypicals (Hazlett et al., 2006; Palmen et al., 2005; Bloss & Courchesne, 2007; Bonhila et al., 2008; Piven et al., 1995; Freitag et al., 2009); however, other studies have reported no differences in lobar volume (Hallahan et al., 2009) or decreases in volume (Rojas et al., 2002; Herbert et al., 2003). Several studies have also documented age-specific alterations to cortical volume (Courchesne et al., 2001; Carper et al., 2002). Disagreement amongst results may be due to varying methods as well as varying ages and types of ASD subjects utilized in each study. Despite this, difficulties delineating between gray and white matter in MRI images may also contribute to conflicting outcomes. Although we cannot directly examine how our results might impact MRI thresholding from these studies, a less distinct gray-white matter transition in the autistic brain could result in a misplaced boundary and subsequent errors in volume and thickness measures, especially when

employing threshold-based tissue parcellation techniques. This issue could be directly assessed in individuals where both postmortem tissue samples and MRI images are available.

3.3 Methodological Considerations

Automated algorithms have been used in a variety of tissue preparations to explore cell patterning. Perhaps most notable in the context of ASD is the Buxhoeveden algorithm (Buxhoeveden et al., 2000), which not only has been utilized to document an increased distance between cortical columns in ASD subjects (Casanova et al., 2002) but also has been applied to dyslexia (Casanova et al., 2002) as well as comparative primate studies (Buxhoeveden & Casanova, 2002). Although these types of algorithms when applied to photomicrographs of the cortex can provide useful information, several caveats should be noted. First, one should strive to approximate a random sampling method. In the present study semi-random selection of regions for examination was determined by a lack of cortical folding while the operator was blind to diagnosis. In addition, the sections selected for analysis were chosen according to stereological sampling principles. Area selection could be automated in an attempt to create a systematic random sample of photomicrographed regions. Second, although we attempted to control for curvature by selecting subjectively noncurved locations, another viable approach might be to quantify the curvature and then partial out its influence on the transition zone measure. Finally, in certain contexts, values acquired automatically from two-dimensional photomicrographs could suffer from bias introduced by the use of nonstereological sampling methods. Although automatic image analysis algorithms may be inappropriate for certain types of neuroanatomical measures, the careful application and interpretation of such measures

provide an avenue for quickly collecting data from neuroanatomical samples and quantifying relative cell patterning differences between subject groups that were previously dependent upon qualitative assessments. Previous approaches to the examination of abnormalities in the subcortical white matter have either been qualitative or have relied upon stereological or nonstereological density counts within the white matter (Conner et al., 2009). This type of approach is potentially problematic given the dramatic decrease in density that occurs with increasing distance from the cortical boundary.

It should also be noted that the current sigmoid fitting method could be extended to other boundaries within the brain as well as other boundaries within the cortex (e.g., layer placement). Sigmoid functions might not be appropriate for less distinct boundaries, but this technique could be extended through the use of multiple data types acquired from the images (i.e., object size, object shape, object distribution) in conjunction with functions that might better model the data from less distinct boundaries (Hutsler and Avino, in prep.). Such an approach to cortical cell patterning abnormalities in ASD has been insufficiently explored.

3.4 Conclusions

These results demonstrate that in the ASD brain, the boundary between gray matter and white matter is not as clearly delineated as it is in neurotypicals. This finding has relevance to claims of neuronal migration disturbances in ASD, as the indistinctiveness of the transition zone may be driven by supernumerary neurons in the subplate. However, the origin of this pattern could also be found in alterations to the developmental apoptosis that is present in the cortical subplate or modifications to the

many factors that influence cell patterning and layer formation in the developing cerebral cortex. In addition, the finding has direct relevance for the interpretation of both MRI volumetric and thickness measure of the cerebral cortex in ASD populations. Finally, the method described in this study could be extended to explore other laminar boundaries within the central nervous system and could prove useful in quantifying other cell patterning abnormalities that could provide insights into cortical development in ASD.

4. Experimental Procedure

All of the cerebral cortical tissue samples utilized in this study were acquired with the assistance of the Autism Tissue Program (ATP, Los Angeles, CA), and all procedures for tissue collection, case identification, and data storage were reviewed by the Biomedical Institutional Review Board at the University of Nevada, Reno. Cortical tissue samples fixed in formalin were acquired from eight male individuals with ASD as well as from eight neurotypical individuals matched for age and sex (see table 1). Identification of the ASD subjects was based upon available medical and psychological records, and the diagnosis was subsequently confirmed with the Revised Autism Diagnostic Inventory (ADI-R; Lord et al., 1994) given to the primary caregiver following tissue donation.

In the present group, all cases met the criteria for a diagnosis of autism except for Case 008 (see table 1), who did not meet the cutoff in the area of communication and was diagnosed as having Asperger's syndrome. For comparison to the ASD cases, control cases were selected based upon age, PMI, and tissue block availability to obtain a final set of eight age- and sex-matched pairs. Control cases had no history of neurological disorders, and brain weights for both groups were collected at autopsy prior to fixation.

From these cases, formalin-fixed cortical tissue samples were obtained from three locations: the lateral surface of the middle temporal gyrus (Brodmann's area 21; posterior middle temporal gyrus, ventral to the termination of the Sylvian fissure), the dorsolateral frontal lobe (Brodmann's area 9; anterior portion of the first frontal convolution, anterior to the premotor cortex, and lateral from the longitudinal fissure by 5 cm), and the dorsal lateral parietal lobe (Brodmann's area 7, superior parietal lobule, posterior but not adjacent to the primary sensory cortex and lateral from the longitudinal fissure by 5 cm).

Tissue block locations were provided to the brain banks using these location descriptors as well as photomicrographs indicating the specific location of the blocks. Following collection, block locations were confirmed with the detailed cytoarchitectonic descriptions provided by von Economo and Koskinas (1925). In several cases, one or more of these regions was unavailable for analysis, and thus, a total of 42 blocks was used in the final study. Tissue blocks were stored in 10% formalin until two weeks prior to processing, when they were transferred to 4% paraformaldehyde. Subsequently, the blocks were cryoprotected in 25% sucrose for 72 hours and cut at a thickness of 50μm on a freezing microtome (American Optical). Every sixth tissue section was mounted onto a gelatin-subbed slide and air dried prior to Nissl staining. Briefly, the sections were dehydrated in a series of alcohols and cleared in toluene. Sections were then rehydrated and transferred into .25% thionin and .4% sodium acetate diluted in .1M phosphate buffer. Sections were then rinsed repeatedly in water prior to dehydrating in a graded series of alcohols and then cleared in toluene. All sections were coverslipped in Permount (Fisher Scientific).

Images of the gray-white matter boundary were acquired using an Olympus BX51 microscope and a Q5 color digital camera (Olympus, Inc). Thirty-two bit (2560x1920 pixel) images of the gray-white matter boundary were taken at final magnification of 100x from segments of the cortical ribbon where there was no curvature. This was achieved by restricting image acquisition to the gyral walls and flat portion of the gyral crown where column orientation was parallel. The boundary between gray and white matter was oriented orthogonally to the long axis of the image and bisected the image area. At each location a measure of total cortical thickness was taken using an eyepiece reticule at a magnification of 40x. These linear measures were taken from the top of cortical layer I to the bottom of cortical layer VI parallel to the orientation of cortical cell columns.

Each image was post-processed using the ImageJ software package (http://rsbweb.nih.gov/ij/). Images were first converted to 8-bit grayscale and then made binary using ImageJ's variation of the iterative intermeans thesholding algorithm described by Ridler and Calverd (1978). Following this procedure, noise and most erythrocytes were removed from each image by removing all objects that were less than 88 μm^2, which eliminated 100% of single erythrocytes and 75% of overlapping erythrocytes.

Sigmoid curves (y = [1/1+e^-bx]) were then overlaid on to each binary image by iteratively searching the image for a "best fit." This procedure required identifying a linear boundary between gray and white matter, which was done using an automated technique. Each image was divided into strips that were perpendicular to the orientation of the boundary, and a count of black pixels was made for each vertical column of the strip and then normalized to a range from zero to one using the maximum pixel count

found in that strip. For each sequence of pixel counts, a sigmoid function with a fixed slope, but varying horizontal offsets, was iteratively moved across the image and the error between the sigmoid and the normalized pixel counts was summed across each column of the image. The center of the sigmoid with the least error was recorded. For each image, six continuous nonoverlapping strips were analyzed across the image, resulting in six best-fit sigmoid centers. Simple linear regression was then used to determine the line of best fit for these six center points. The resulting line was used to correct any gray-white matter boundary misalignments by recording the resulting angle of each regression line and then adjusting for the rotational error. A single best-fit sigmoid was then fit to the entire image. This was achieved by counting all of the pixels in a one pixel column-wide fashion across the image. These pixel counts were smoothed using a moving average across the image that was 111 μm wide and then normalized to a range from zero to one using the maximum pixel count found in each image. Sigmoid functions with varying slopes and offsets were iteratively fit to this trace, and the offset and slope with the lowest error were automatically recorded.

A 2 x 3 mixed-model analysis of variance was used to evaluate the difference between autistic subjects' and control subjects' sigmoid slopes for the three regions examined (BA7, BA9, and BA21). To assess the influence of other potentially relevant subject characteristics, age, postmortem interval, and brain weight were included in the model as covariates. Finally, seizure activity and level of cognitive functioning were qualitatively assessed alongside each subjects boundary measure.

References

Alghoul, W.M., Miller, M.W., 1989. Transient expression of ALZ-50 immunoreactivity in developing rat neocortex – a marker for naturally-occurring neuronal death. Brain Res. 481**,** 361-367.

Bailey, A., Luthert, P., Dean, A., Harding, B., Janota, I., Montgomery, M., Rutter, M., Lantos, P., 1998. A clinicopathological study of autism. Brain. 121**,** 889-905.

Bailey, P., von Bonin, G., 1951. The Isocortex of Man, University of Illinois Press, Urbana.

Battaglia, G., Arcelli, P., Granata, T., Selvaggio, M., Andermann, F., Dubeau, F., Olivier, A., Tampieri, D., Villemure, J.G., Avoli, M., Avanzini, G., Spreafico, R., 1996. Neuronal migration disorders and epilepsy: A morphological analysis of three surgically treated patients. Epilepsy Res. 26**,** 49-58.

Bauman, M., Kemper, T.L., 1985. Histoanatomic observations of the brain in early infantile-autism. Neurology. 35**,** 866-874.

Bloss, C.S., Courchesne, E., 2007. MRI neuroanatomy in young girls with autism: A preliminary study. J. Am. Acad. Child and Adolesc. Psy. 46**,** 515-523.

Boddaert, N., Chabane, N., Gervais, H., Good, C.D., Bourgeois, M., Plumet, M.H., Barthelemy, C., Mouren, M.C., Artiges, E., Samson, Y., Brunelle, F., Frackowiak, R.S.J., Zilbovicius, M., 2004. Superior temporal sulcus anatomical abnormalities in childhood autism: a voxel-based morphometry MRI study. Neuroimage. 23**,** 364-369.

Bonilha, L., Cendes, F., Rorden, C., Eckert, M., Dalgalarrondo, P., Li, L.M., Steiner, C.E., 2008. Gray and white matter imbalance - Typical structural abnormality underlying classic autism? Brain Dev. 30**,** 396-401.

Bushong, E.A., Martone, M.E., Ellisman, M.H., 2003. Examination of the relationship between astrocyte morphology and laminar boundaries in the molecular layer of adult dentate gyrus. J. Comp. Neurol. 462**,** 241-251.

Buxhoeveden, D.P., Switala, A.E., Roy, E., Casanova, M.F., 2000. Quantitative analysis of cell columns in the cerebral cortex. J. Neurosci. Methods. 97**,** 7-17.

Buxhoeveden, D.P., Casanova, M.F., 2002. The minicolumn and evolution of the brain. Brain Behav. Evol. 60**,** 125-151.

Canitano, R., 2007. Epilepsy in autism spectrum disorders. Eur. Child Adolesc. Psychiatry. 16**,** 61-66.

Carper, R.A., Moses, P., Tigue, Z.D., Courchesne, E., 2002. Cerebral lobes in autism: Early hyperplasia and abnormal age effects. Neuroimage. 16**,** 1038-1051.

Casanova, M.F., Buxhoeveden, D.P., Switala, A.E., Roy, E., 2002. Minicolumnar pathology in autism. Neurology. 58**,** 428-432.

Chugani, D.C., 2004. Serotonin in autism and pediatric epilepsies. Ment. Retard. Dev. D. R. 10**,** 112-116.

Chun, J.J.M., Shatz, C.J., 1989. Interstitial-cells of the adult neocortical white matter are the remnant of the early generated subplate neuron population. J. Comp. Neurol. 282**,** 555-569.

Chung, M.K., Robbins, S.M., Dalton, K.M., Davidson, R.J., Alexander, A.L., Evans, A.C., 2005. Cortical thickness analysis in autism with heat kernel smoothing. Neuroimage. 25**,** 1256-1265.

Connor, C.M., Guo, Y., Akbarian, S., 2009. Cingulate white matter neurons in Schizophrenia and Bipolar Disorder. Biol. Psychiatry. 66**,** 486-493.

Courchesne, E., 1988. Cerebellar changes in autism, in: Swann, J. W., Messer , A. (Eds.), Albany Birth Defects Symposium, 18. Disorders of the Developing Nervous System: Changing Views on Their Origins, Diagnoses, and Treatments. Alan R. Liss, Inc., Albany, NY, pp. 93-110.

Courchesne, E., Karns, C.M., Davis, H.R., Ziccardi, R., Carper, R.A., Tigue, Z.D., Chisum, H.J., Moses, P., Pierce, K., Lord, C., Lincoln, A.J., Pizzo, S., Schreibman, L., Haas, R.H., Akshoomoff, N.A., Courchesne, R.Y., 2001. Unusual brain growth patterns in early life in patients with autistic disorder - An MRI study. Neurology. 57**,** 245-254.

Fatemi, S.H., Stary, J.M., Egan, E.A., 2002. Reduced blood levels of reelin as a vulnerability factor in pathophysiology of autistic disorder. Cell. Mol. Neurobio. 22**,** 139-152.

Fatemi, S.H., Snow, A.V., Stary, J.M., Araghi-Niknam, M., Reutiman, T.J., Lee, S., Brooks, A.I., Pearce, D.A., 2005. Reelin signaling is impaired in autism. Biol. Psychiatry. 57**,** 777-787.

Freitag, C.M., Luders, E., Hulst, H.E., Narr, K.L., Thompson, P.M., Toga, A.W., Krick, C., Konrad, C., 2009. Total brain volume and corpus callosum size in medication-naive adolescents and young adults with autism spectrum disorder. Biol. Psychiatry. 66**,** 316-319.

Hadjikhani, N., Joseph, R.M., Snyder, J., Tager-Flusberg, H., 2006. Anatomical differences in the mirror neuron system and social cognition network in autism. Cereb. Cortex. 16**,** 1276-1282.

Hallahan, B., Daly, E.M., McAlonan, G., Loth, E., Toal, F., O'Brien, F., Robertson, D., Hales, S., Murphy, C., Murphy, K.C., Murphy, D.G.M., 2009. Brain morphometry volume in autistic spectrum disorder: a magnetic resonance imaging

study of adults. Psychol. Med. 39**,** 337-346.

Hardan, A.Y., Minshew, N.J., Mallikarjuhn, M., Keshavan, M.S., 2001. Brain volume in autism. J. Child Neurol. 16**,** 421-424.

Hardan, A.Y., Muddasani, S., Vemulapalli, M., Keshavan, M.S., Minshew, N.J., 2006. An MRI study of increased cortical thickness in autism. Am. J. Psychiatry. 163**,** 1290-1292.

Hazlett, H.C., Poe, M., Gerig, G., Smith, R.G., Provenzale, J., Ross, A., Gilmore, J., Piven, J., 2005. Magnetic resonance imaging and head circumference study of brain size in autism - birth through age 2 years. Arch. Gen. Psychiatry. 62**,** 1366-1376.

Hazlett, H.C., Poe, M.D., Gerig, G., Smith, R.G., Piven, J., 2006. Cortical gray and white brain tissue volume in adolescents and adults with autism. Biol. Psychiatry. 59**,** 1-6.

Herbert, M.R., Ziegler, D.A., Deutsch, C.K., O'Brien, L.M., Lange, N., Bakardjiev, A., Hodgson, J., Adrien, K.T., Steele, S., Makris, N., Kennedy, D., Harris, G.J., Caviness, V.S., 2003. Dissociations of cerebral cortex, subcortical and cerebral white matter volumes in autistic boys. Brain. 126**,** 1182-1192.

Hevner, R.F., Shi, L.M., Justice, N., Hsueh, T.P., Sheng, M., Smiga, S., Bulfone, A., Goffinet, A.M., Campagnoni, A.T., Rubenstein, J.L.R., 2001. Tbr1 regulates differentiation of the preplate and layer 6. Neuron. 29**,** 353-366.

Hutsler, J.J., Love, T., Zhang, H., 2007. Histological and magnetic resonance imaging assessment of cortical layering and thickness in autism spectrum disorders. Biol. Psychiatry. 61**,** 449-457.

Hutsler, J.J., Zhang, H., 2010. Increased dendritic spine densities on cortical projection neurons in autism spectrum disorders. Brain Res. 1309**,** 83-94.

Janusonis, S., Gluncic, V., Rakic, P., 2004. Early serotonergic projections to Cajal-Retzius cells: Relevance for cortical development. J. Neurosci. 24**,** 1652-1659.

Kemper, T.L., 1988. Neuroanatomic studies of dyslexia and autism, in: Swann, J. W., Messer, A. (Eds.), Albany Birth Defects Symposium, 18. Disorders of the Developing Nervous System: Changing Views on Their Origins, Diagnoses, and Treatments. Alan R. Liss, Inc., Albany, NY, pp. 125-154.

Kemper, T.L., 2010. The developmental neuropathology of autism, in G. Blatt (Ed.), The neurochemicals basis of autism. Springer, New York, pp. 69-82.

Lord, C., Rutter, M., LeCouteur, A., 1994. Autism Diagnostic Interview-Revised: A revised version of a diagnostic interview for caregivers of individuals with possible pervasive developmental disorders. J. Autism Dev. Disord. 24, 659-685.

Marin-Padilla, M., 1998. Cajal-Retzius cells and the development of the neocortex. Trends Neurosci. 21**,** 64-71.

McAlonan, G.M., Cheung, V., Cheung, C., Suckling, J., Lam, G.Y., Tai, K.S., Yip, L., Murphy, D.G.M., Chua, S.E., 2005. Mapping the brain in autism. A voxel-based MRI study of volumetric differences and intercorrelations in autism. Brain. 128**,** 268-276.

McAlonan, G.M., Suckling, J., Wong, N., Cheung, V., Lienenkaemper, N., Cheung, C., Chua, S.E., 2008. Distinct patterns of grey matter abnormality in high-functioning autism and Asperger's syndrome. J. Child Psychol. Psychiatry. 49**,** 1287-1295.

McConnell, S.K., Ghosh, A., Shatz, C.J., 1994. Subplate pioneers and the formation of descending connections from cerebral cortex. J. Neurosci. 14**,** 1892-1907.

Mennerick, S., Zorumski, C.F., 2000. Neural activity and survival in the developing nervous system. Mol. Neurobiol. 22**,** 41-54.

Muhle, R., Trentacoste, S.V., Rapin, I., 2004. The genetics of autism. Pediatrics. 113**,** E472-E486.

Newschaffer, C.J., Croen, L.A., Daniels, J., Giarelli, E., Grether, J.K., Levy, S.E., Mandell, D.S., Miller, L.A., Pinto-Martin, J., Reaven, J., Reynolds, A.M., Rice, C.E., Schendel, D., Windham, G.C., 2007. The epidemiology of autism spectrum disorders. Annu. Rev. Public Health. 28**,** 235-258.

Nomura, T., Takahashi, M., Hara, Y., Osumi, N., 2008. Patterns of neurogenesis and amplitude of reelin expression are essential for making a mammalian-type cortex. Plos One. 3.

Palmen, S., Pol, H.E.H., Kemner, C., Schnack, H.G., Durston, S., Lahuis, B.E., Kahn, R.S., Van Engeland, H., 2005. Increased gray-matter volume in medication-naive high-functioning children with autism spectrum disorder. Psychol. Med. 35**,** 561-570.

Piven, J., Berthier, M.L., Starkstein, S.E., Nehme, E., Pearlson, G., Folstein, S., 1990. Magnetic resonance imaging evidence for a defect of cerebral cortical development in autism. Am. J. Psychiatry. 147**,** 734-739.

Piven, J., Arndt, S., Bailey, J., Havercamp, S., Andreasen, N.C., Palmer, P., 1995. An MRI study of brain size in autism. Am. J. Psychiatry. 152**,** 1145-1149.

Puelles, L., Rubenstein, J.L.R., 2003. Forebrain gene expression domains and the evolving prosomeric model. Trends Neurosci. 26**,** 469-476.

Rapin, I., 1997. Autism. N. Engl. J. Med. 337**,** 97-104.

Rice, D., Barone, S., 2000. Critical periods of vulnerability for the developing nervous system: Evidence from humans and animal models. Environ. Health Perspect.

108**,** 511-533.

Rice, D.S., Curran, T., 2001. Role of the reelin signaling pathway in central nervous system development. Annu. Rev. Neurosci. 24**,** 1005-1039.

Ridler, T.W., Calvard, S., 1978. Picture thresholding using an iterative selection method. Ieee T. Syst. Man Cyb. 8**,** 630-632.

Rojas, D.C., Bawn, S.D., Benkers, T.L., Reite, M.L., Rogers, S.J., 2002. Smaller left hemisphere planum temporale in adults with autistic disorder. Neurosci. Lett. 328**,** 237-240.

Serajee, F.J., Zhong, H.L., Huq, A., 2006. Association of reelin gene polymorphisms with autism. Genomics. 87**,** 75-83.

Simms, M.L., Kemper, T.L., Timbie, C.M., Bauman, M.L., Blatt, G.J., 2009. The anterior cingulate cortex in autism: heterogeneity of qualitative and quantitative cytoarchitectonic features suggests possible subgroups. Acta Neuropathol. 118**,** 673-684.

Skaar, D.A., Shao, Y., Haines, J.L., Stenger, J.E., Jaworski, J., Martin, E.R., DeLong, G.R., Moore, J.H., McCauley, J.L., Sutcliffe, J.S., Ashley-Koch, A.E., Cuccaro, M.L., Folstein, S.E., Gilbert, J.R., Pericak-Vance, M.A., 2005. Analysis of the RELN gene as a genetic risk factor for autism. Mol. Psychiatry, 10**,** 563-571.

von Economo, C., Koskinas, G. 1925. Die Cytoarchitektonik der Hirnrinde des erwachsenen Menschen. Julius Springer Verlag, Berlin.

Whitney, E.R., Kemper, T.L., Bauman, M.L., Rosene, D.L., Blatt, G.J., 2008. Cerebellar Purkinje cells are reduced in a subpopulation of autistic brains: A stereological experiment using Calbindin-D28k. Cerebellum. 7**,** 406-416.

Zhang, H., Liu, X., Zhang, C., Mundo, E., Macciardi, F., Grayson, D. R., Guidotti, A. R., Holden, J. J. A., 2002. Reelin gene alleles and susceptibility to autism spectrum disorders. Mol. Psychiatry, 7, 1012-1017.

Appendix A: Tables

Table 1 – Case Information

Case ID	Diagnosis	R/L	Age	PMI (hrs)	Brain Wgt (gms)	Brodmann Area 7	9	21	Cause of Death
001	ASD	R	10	30	900*	X	X	X	Drowning
002	ASD	R	20	24	1140	X	X		Motor Vehicle Accident
003	ASD	L	25	26	1220	X	X		Seizure
004	ASD	R	27	8	1720	X	X	X	Drowning
005	ASD	L	29	24	1340	X	X	X	Cardiac Arrhythmia
006	ASD	R	32	21	1710	X	X	X	Congestive Heart Failure
007	ASD	R	44	31	1530	X	X	X	Myocardial Infarction
008	ASD	L	45	20	1370	X	X	X	Pulmonary Embolism
Means			29	23.0	1366				
009	Control	R	11	20	1420	X	X		Internal Bleeding
010	Control	L	17	6.5	1240	X	X	X	Trauma
011	Control	L	22	24	1580	X	X	X	Motor Vehicle Accident
012	Control	R	27	21	1330	X	X	X	Asphyxiation/Hanging
013	Control	L	27	16	NA	X	X		Arteriosclerosis
014	Control	L	29	24*	1350	X			Gunshot Wounds
015	Control	L	43	24	1450	X	X	X	Cardiovascular Disease
016	Control	L	51	24	1600	X	X	X	Myocardial Infarction
Means			28.4	19.9	1424				

* = Estimated   NA = Not available

Table 2. Correlation Table

	r	N of pairs	p
Age x PMI	.254	8	NS
Age x Brain Weight	**.520**	**7**	**.047**
Age x Sigmoid Slope	.446	8	NS
PMI x Brain Weight	-.357	7	NS
PMI x Sigmoid Slope	.356	8	NS
Brain Weight x Sigmoid Slope	.365	7	NS

Appendix B: Figures

Figure 1. Quantification of the transition zone between cortical gray and white matter using overlaid sigmoid functions in binary images. Neurotypical subjects (A) boundaries were typically more distinct than those found in ASD subjects (B). Scale bar = 100μm.
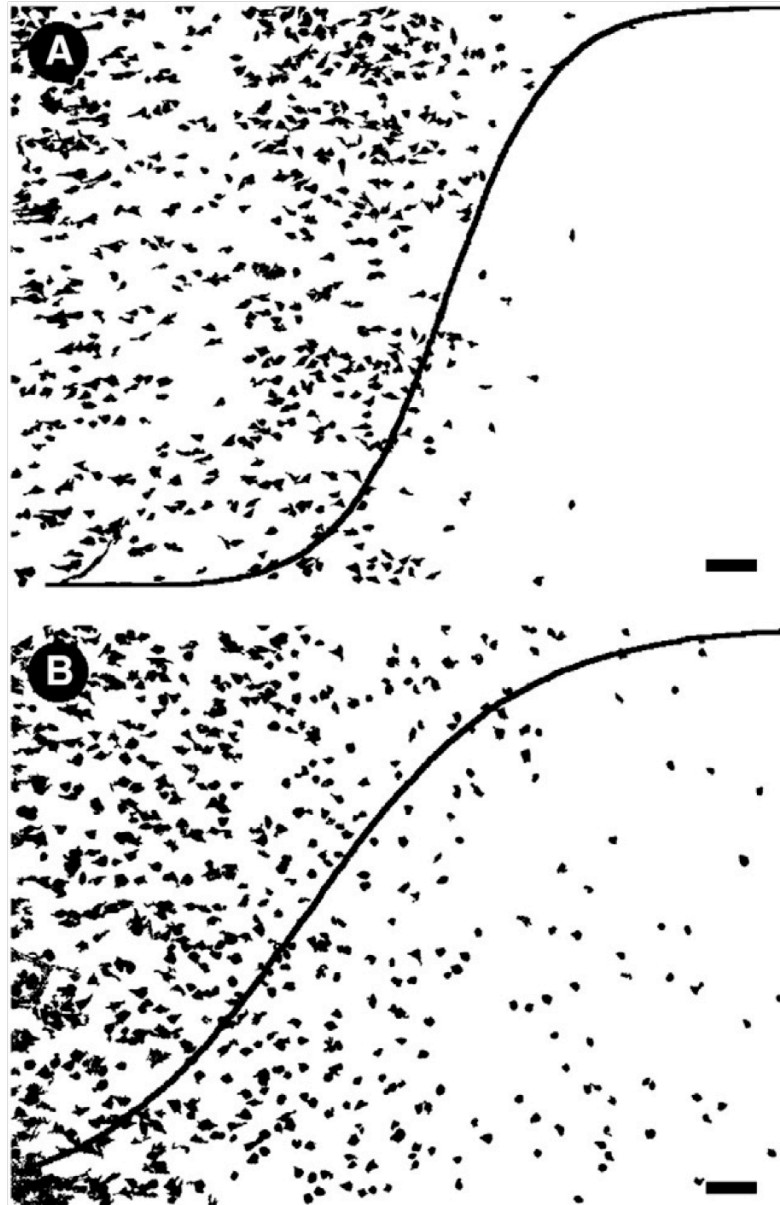
Figure 2. Sigmoid slope value comparisons between ASD and neurotypical subjects within eulaminate isocortex taken from frontal (BA9), parietal (BA7), and temporal (BA 21) lobe locations. In all three cortical regions examined ASD subjects showed shallower (higher) sigmoid slope values as compared to neurotypicals. Error bars indicate the standard error of the mean.
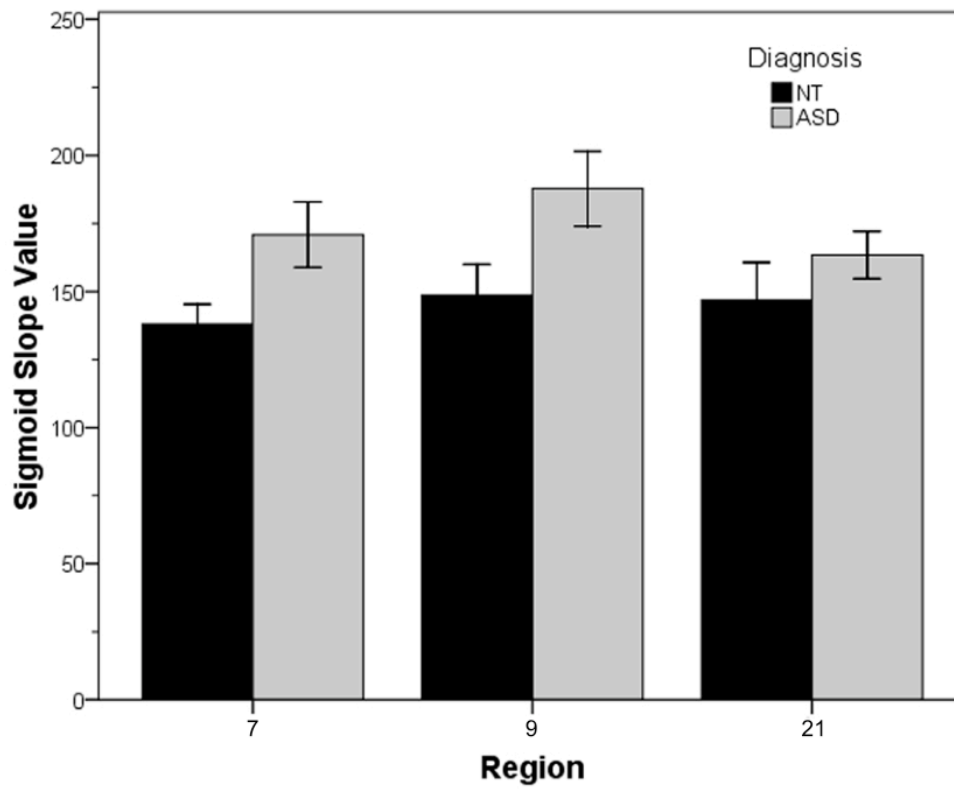
Figure 3. Average angle of the sigmoid slope values (corrected for in-plane image tilt) collected from each subject irrespective of cortical location. In seven of the eight ASD cases examined, the angles of the sigmoid slopes were shallower than the mean angle of the control cases. Horizontal line indicates the average angle of the sigmoid slopes of the eight neurotypical subjects. NT = Neurotypical; ASD = Autism Spectrum Disorder